Effect of the Extensional Flow on the Properties of Oriented Nanocomposite Films for Twist Wrapping

Nadka Tzankova Dintcheva, Rosamaria Marino, Francesco Paolo La Mantia

Dipartimento di Ingegneria Chimica dei Processi e dei Materiali, Università di Palermo, Viale delle Scienze, Palermo 90128, Italy

Received 19 February 2010; accepted 9 August 2010
DOI 10.1002/app.33354
Published online 10 January 2011 in Wiley Online Library (wileyonlinelibrary.com).

ABSTRACT: In this study, we examined the mechanical behavior of nanocomposite films based on polyethylene (PE) and pristine PE films. The films were prepared by film blowing and were then cold-drawn at low temperature. The experimental results show that cold drawing significantly enhanced the orientation; with increasing draw ratio (DR), the elastic modulus and tensile strength of the PE films strongly increased, particularly in the presence of the organoclay. To obtain polymeric films suitable for twist wrapping, the films must be sufficiently stiff so that no shrinkage or elastic recovery occur during or after twisting. The elongation at break and the yield strain sharply decreased with orientation, mainly in films upon drawing. According to the mechanical behavior, the twist angle increased with increasing DR and, particularly, with the addition of nanoclay, probably because of the applied DR, which reduced the nanoparticle size and, as a consequence, hindered the applied torsional elastic recovery. Therefore, the nanocomposite film with a higher DR was particularly suitable for twist-wrapping applications. © 2011 Wiley Periodicals, Inc. J Appl Polym Sci 120: 2772–2779, 2011

Key words: twist wrapping; polyethylene-based nanocomposite film; clay particles

INTRODUCTION

Food packaging is one of the key factors in the preservation of food products and their marketing. In recent decades, the use of plastics in this area has increased greatly, and this has amplified the attention of researchers in the polymer field. These studies have mainly been devoted to improving the mechanical and barrier properties, freshness preservation, and to improving the production-processes monitoring of the environmental impact.

Particular interest has been devoted to plastic films for the packaging twists of sweets such as candies, chocolates, and Torron. The main characteristics of these films are essentially the maintenance of the applied twist, good barrier properties, flexibility, tear and puncture, no chemical interaction with food, and so on. Twist wrapping is a particular method of closing-complete wrappings for the packaging of goods. A prerequisite for the use of twist wrapping is the suitability of the film, which must be sufficiently stiff so that no shrinkage or elastic recovery occur during or after twisting, respectively.

According to the literature, cellophane, that is, regenerated cellulose, oriented polypropylene, and poly(vinyl chloride) films are predominantly used for candy wrapping.[1,2]

Polyethylene (PE) is one of the most widely used polyolefin polymers, and interest in it in food packaging is emerging because of its low cost, excellent moisture barrier properties, and easy processability. Most schemes to improve the PE gas barrier properties involve either the addition of higher barrier plastics via a multilayer structure or high barrier surface coatings; however, these approaches are not cost effective.[2] The growing field of polymer-layered nanocomposites is unique in that it addresses the shortcomings of polyolefins for both packaging and engineered applications requiring desirable mechanical, thermal, and good barrier properties. The incorporation of nanofillers, such as organomodified montmorillonite or bentonite, enhances the mechanical, thermomechanical, and optical properties. Indeed, in the field of plastics, nanocomposite materials are understood as polymer formulations that incorporate finely dispersed particles, such as clay minerals, into the polymer matrix. The relevant aspect is that the particles are mixed within the polymer and then dispersed. The properties of such nanocomposites have already been published in numerous publications. It is known that finely dispersed clay minerals provide the nanocomposite with improved properties, such as increased mechanical strength and enhanced barrier properties against gas molecules (water, oxygen, carbon dioxide,

Correspondence to: N. T. Dintcheva (dintcheva@dicpm.unipa.it).

or aromatics through the packaging materials). The most commonly used mineral in nanocomposites is organically modified montmorillonite.[3–18]

The thermal instability of ammonium-modified montmorillonite, also at low polymer processing temperatures, has drawn the attention of the scientific and industrial communities,[12,14–18] and new alternative methods to control the number of layers of dispersed silicate platelets have been reported in the literature.[19–22] In particular, two different ways have been followed: first, the formulation of a new, more thermally stable organomodifier, such as with pyridinium-modified clays,[19] and second, the self-assembling of nanoparticles, for example, the talc/talc/smectite particle composition.[20] Actually, the industrial applications of these innovative nanofillers are limited.

In this study, the effect of the extensional flow on the properties of oriented PE and PE/Cloisite 15A (CL) films was investigated. Also, the synergic effects of cold drawing and clay presence on the morphology modification, mechanical performance, and suitability for twist-wrapping application of these films were analyzed and are discussed.

EXPERIMENTAL

Materials

A commercially available film-grade linear low-density PE (Clearflex FG166, weight-average molecular weight = 130,000 g/mol, weight-average molecular weight/number-average molecular weight = 3.8, melt flow index at 190°C and 2.16 kg = 0.27 g 10/min, and density = 0.918 g/cm^3 at room temperature; Polimeri Europa, Priolo, Italy) and an organomodified clay sample (CL, from Southern Caly products, Conzales, TX, USA) were used. CL was a ditallowdimethylammonium-modified montmorillonite with an average diameter of 8 μm; the organomodifier concentration was 125 mequiv/100 g of clay. Hydrogenated tallow of CL was a blend of saturated *n*-alkyl groups with an approximate composition of 65% C18, 30% C16, and 5% C14.

Compounding and film blowing

Linear low-density PE was compounded with 5 wt % organoclay in a corotating intermeshing twin-screw extruder (OMC, Roddi (Cuneo), Italy; diameter = 19 mm, length-to-diameter ratio = 35) with the thermal profile 120–140–150–160–170–180°C and a mixing speed of 220 rpm. For comparison, the pure polymer underwent the same extrusion process. The residence time was about 90–110 s.

The films were obtained by a single-screw extruder equipped with a film-blowing head and a Brabender (Duisburg, Germany) film blowing unit. The temperature profile was 120–140–170–190°C, and the screw speed was 70 rpm. The drawing speed of the film was kept constant at about 4 m/min. The final thickness of the films was about 95 μm.

The films were cold-drawn with the aid of an Instron dynamometer model 3365 equipped with wooden clamps at room temperature and at a crosshead speed of 200 mm/min. The initial length (L_0) was 30 mm in all cases. The amount of drawing was characterized by the draw ratio (DR = L_f/L_0), where L_f is the final length.

Characterization

A capillary viscometer (Rheologic 1000, CEAST, Turin, Italy) equipped with a drawing system was used to investigate the rheological behavior in nonisothermal elongational flow. The capillary diameter was 1 mm, and the length-to-diameter ratio was 40. The force in the molten filament at breaking was measured directly and is known as *melt strength* (MS). The breaking–stretching ratio (BSR) was calculated as the ratio between the drawing speed at breaking and the extrusion velocity at the die. The data were collected at 160°C.

Mechanical tests were carried out with the same universal Instron machine model 3365 according to ASTM test method D 882. The specimens were cut from films in the machine direction. The modulus was measured at a speed of 1 mm/min. When the deformation was about 10%, the speed was increased to 200 mm/min until break. The data reported, elastic modulus (E), tensile strength (TS), elongation at break (EB), and deformation yield point, are the average values obtained by analysis of the results of seven tests per sample in the machine direction of all of the films. The reproducibility of the results was about ±5% from the average. The measurements were performed in the machine direction of the film. Testing the sample in the transverse direction was not possible because a significant reduction of the film surface after the draw was observed.

Suitability for twist wrapping was investigated by the application of a twist of 360° clockwise. After twisting, the maintenance angle (θ*) as a function of the time was calculated with the following formula:

$$\theta^* = [(\theta_0 - \theta_t)/\theta_0] \times 100$$

where θ_0 is the beginning angle and θ_t is the angle at a given time.

Wide-angle X-ray analyses were performed at room temperature in the reflection mode on a Siemens D-500 (Houghiton, MI) D-500 X-ray diffractometer with Cu Kα radiation with a wavelength of 0.1542 nm. A scanning rate of 10°/min was used.

TABLE I
MS, BSR, and Main Mechanical Properties (*E*, TS, and EB) of the PE and PE/CL Samples

	MS (cN)[a]	BSR[a]	*E* (MPa)	TS (MPa)	EB (%)
PE	3.6	39	141	27	722
PE/CL	4.2	35	162	26	715

[a]At an apparent shear rate of 60 1/s.

The interlayer distances (d_{001}'s) in all of the OMMT-filled blend systems was carried out according to Bragg's formula:

$$d_{001} = n\lambda/(2\sin\theta)$$

where n is an integer, λ is the wavelength, and θ is the angle of incidence of the X-ray beam.

Scanning electron microscopy (SEM) analysis was performed by scanning of the fracture surface of some samples by means of a Philips ESEM XL30, Delft, The Netherlands.

RESULTS AND DISCUSSION

To evaluate their ability to form films, MS and BSR of the unfilled and clay-filled films in a nonisothermal elongational flow were measured. The nonisothermal elongational flow is involved in film-blowing operation, and the MS and BRS values give a useful indication of the filmability (ability to form film) of the molten polymer systems. In Table I (first and second column), the measured values of MS and BSR at a 60 s^{-1} apparent shear rate are reported. Generally, the processability in elongational flow improves with increasing values of MS and BSR. In effect, with the addition of the clay nanoparticles, the resistance to break in the melt increased, and this increase was about 17% more than the unfilled PE, whereas the reduction in BSR at same apparent shear rate was less than 9% with respect to the PE one. This slight reduction of BSR did not compromise the film-blowing operation. The increase in MS and the subsequent significant decrease in BSR for conventional filled polymers are usually correlated with reduced stretchability in these materials.[23,24] However, with the addition of the clay nanoparticles at this relatively high filler concentration, the resistance to the break in the melt increased; this indicated an improved stretchability of the system.

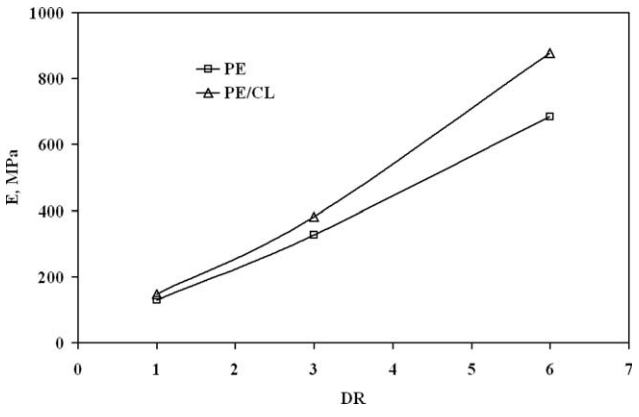

Figure 1 *E* as a function of DR of the pristine PE and PE/CL films.

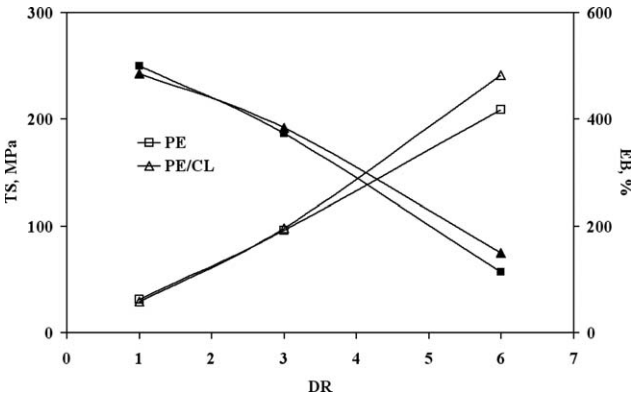

Figure 2 TS (empty symbols) and EB (full symbols) as a function of the DR values of the pristine PE and PE/CL films.

In the light of the obtained results in the nonisothermal elongational flow and our previous experience in clay-filled fiber preparation in extensional flow,[25–27] oriented nanocomposite films for twist wrapping were prepared. The mechanical performances, in particular, *E*, TS, and EB, of the PE and PE/CL films as a function of DR were measured, and in Figures 1 and 2, the trends of these mechanical properties are shown. Also, in Table I, the main mechanical properties of the compression-molded sheets of the PE and PE/CL samples, that is, the nonoriented samples, are reported. The clay presence for the compression-molded sample, in agreement with ray data reported in the literature,[3–18,23–27] increased *E*, whereas the properties at break were almost unchanged. The increase in *E* for the nonoriented PE/CL sample with respected to the unfilled PE was about 15%; this was similar to the rise of the film at low DR (DR1, where DR1 indicates a film that was not subjected to drawing). Therefore, with application of the extensional flow, the difference between the unfilled and filled samples increased; that is, the increases in the *E* values of the PE/CL film were about 17 and 28% more than in the unfilled PE film for DR3 and DR6, respectively (see Fig. 1).

For the properties at break (see Fig. 2), with clay addition, TS was almost unchanged for the compression-molded sample and for the oriented sample at low DR, that is, DR1 and DR3. Furthermore, TS of the PE/CL film increased about 15% with respect to the PE film at high DR, DR6. The clay presence did not significantly influence EB until low DR. It is interesting to highlight that the

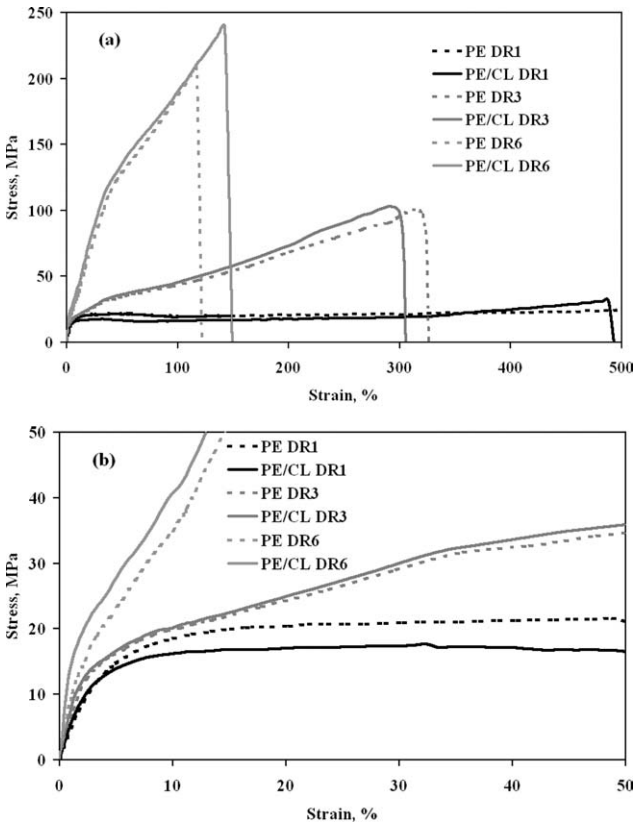

Figure 3 Stress–strain curves of the pristine PE and PE/CL films at different DRs, that is, DRs = 1, 3, and 6.

higher oriented PE/CL film, DR6, showed a significantly higher value of EB than the PE film.

Therefore, the beneficial effect on the mechanical performance for the oriented films was not only due to the orientation of the macromolecules, but it was also due to the some interaction between the oriented macromolecules and the clay nanoparticles. In our previously studies, by birefringence and calorimetric analysis, we demonstrated that the same orientation of the macromolecules of the unfilled and filled fibers occurs. Moreover, we suppose that the orientation of the macromolecules in the film formulation, at same DR, did not change because of the clay presence, as in fiber formulation.[25,26]

To better understand the effect of the extensional flow on the mechanical performances of PE and PE/CL films, typical stress–strain curves at different DRs, that is, 1, 3, and 6, are shown in Figure 3(a). As expected, with increasing orientation of both unfilled and filled films, EB decreased and significantly increased the stress values. The same stress–strain curves at low strain values are reported in Figure 3(b). It was evident that the clay particles caused a strong upturn in the curves; that is, the PE/CL film was more rigid than the pristine PE film, and this effect was more pronounced at high orientation. Also, with the clay presence, some reduction of deformation at yield point values was observed. The last fact was very important; it was the determinant and/or discriminating factor for the film in twist-wrapping applications. The value of the deformation at yield point was so much lower, and the suitability of the film for twist-wrapping applications was so much better. In Table II, the strain at yield point values of the compression-molded samples and oriented unfilled and clay filled films are reported. The clay presence reduced the values of the deformation at yield point more than the values of the pristine samples, and this reduction was more pronounced at high orientation; in particular, at DR = 6, the yield point was not noticed.

Also, to evaluate the film suitability for twist wrapping, the measurements of the maintenance (twist) angle were carried out, and in Figure 4(a), the calculated θ* values as a function of time are reported.

Now, the unfilled PE film showed improved suitability for twist wrapping with increasing orientation. With the clay presence, the ability in film formation for twist wrapping increased even more. The higher oriented PE/CL film (DR6) appeared to be the most suitable for twist-wrapping applications compared to all of the other films. In Figure 4(b), the θ* values of the unfilled PE and PE/CL films at DR = 6 and the θ* values of two unfilled commercial twist-wrapping PE films (FC1 and FC2) are reported. The higher oriented PE/CL film showed the ability to maintain twist wrapping in a manner similar to the commercial oriented sample. The clay presence, in particular, at low loading, allowed the formation of an inexpensive (cheap) film with good mechanical performance and suitability for twist-wrapping applications.

The change in the clay morphology upon the extensional flow was also examined. In Figure 5, the X-ray trace and, in Table III, the calculated d_{001}'s with Bragg's formula of the pristine clay and oriented PE/CL films are reported. d_{001} increased with increasing DR; this suggested that the extensional flow was able to induce some clay morphology modification. Furthermore, the X-ray trace of the pristine clay showed well-distinguished peaks between 2 and 4° and a small shoulder between 6 and 8° due to second diffraction order. The peak

TABLE II
Strain at Yield Point of the Compression-Molded PE and PE/CL Samples and the PE and PE/CL Films at Different DRs

	PE film	PE/CL film
Compression-molded sample	62	60
DR1	41	35
DR3	15	10
DR6	—	—

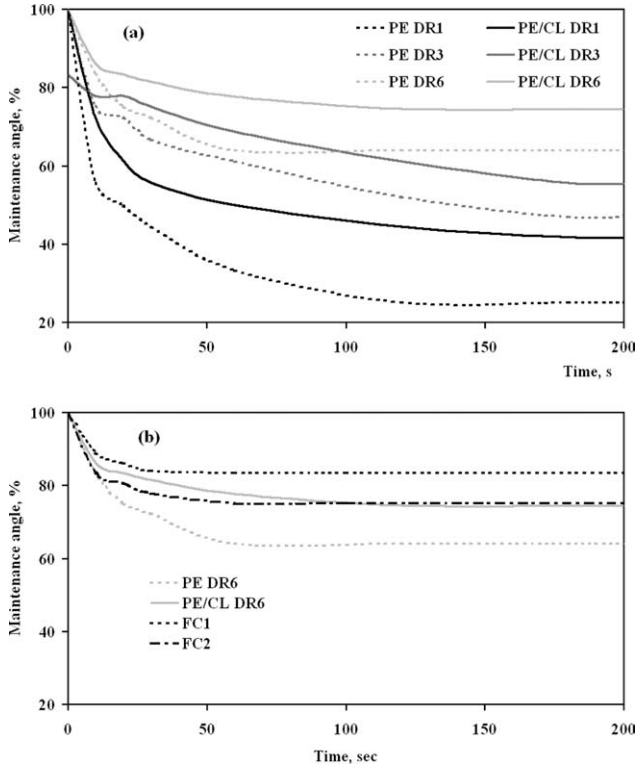

Figure 4 θ* values of the (a) pristine PE and PE/CL films at different DRs, that is, DRs = 1, 3, and 6, and (b) two unfilled commercial twist wrapping PE films.

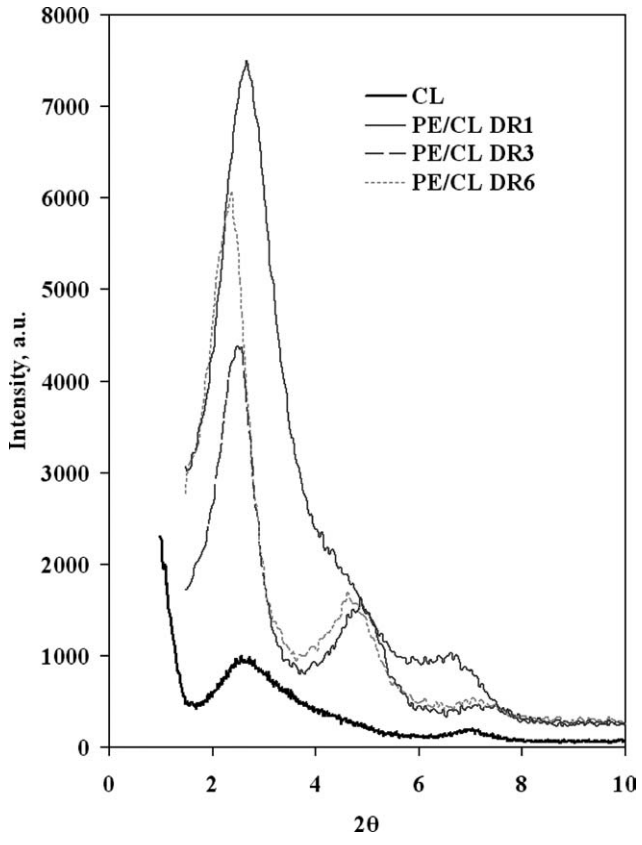

Figure 5 X-ray traces of the pristine clay and PE/CL films at different DRs, that is, DRs = 1, 3, and 6.

TABLE III
Main Peaks and d_{001} of the Pristine Clay and PE/CL Films at Different DRs

	Peak (2θ)	d_{001}
CL	2.80	3.15
PE/CL DR = 1	2.66	3.30
PE/CL DR = 3	2.47	3.57
PE/CL DR = 6	2.37	3.71

positions of the unoriented PE/CL film (DR = 1) were similar (see the values reported in Table III), but the peak intensities were different; this suggested better dispersion of the clay particles without significant intercalation. For the oriented PE/CL films, DR = 3 and 6; another peak between the 4 and 6° appeared, which was in agreement with the literature; the presence of this peak was correlated with the loss of mass from the organoclay galleries. The hypothesis about the gas formation was, however, acceptable because the degradation of the organomodifier followed Hoffmann's elimination reaction and, in particular, occurred with the formation of α-olefins, amines, and other secondary products.[12,14–18]

Finally, the accurate SEM analysis of all of the samples were reformed, and in Figures 6–8, the micrographs at different magnifications are shown. The micrographs of PE/CL sample before film formulation showed a very poor morphology (see Fig. 6). Nonadhesion between the clay and matrix was observed; that is, a great number of the clay particles were detached by the PE matrix. Also, the dimensions of the clay particles were a few micrometers, and the distribution was completely irregular. Also, the micrographs of the PE/CL film before drawing clearly indicated the pour morphology formation (see Fig. 7, DR1 in the first row shows the reported micrographs at different magnifications). The clay particles of the PE/CL film were not uniformly distributed and were separated from the polymer matrix, and also, some holes were observed. This last observation could be explained because the clay degradation occurred during processing (following the Hoffman elimination, that is, the formation of α-olefins and amines) and gave rise to some output of secondary products at low molecular weight; this resulted from the secondary reactions between the degradation products into the clay.[12,14–17] An improved morphology with increasing DR for the PE/CL film was observed; in particular, at higher DRs, that is, DR6, the clay distribution and adhesion between the matrix and particles appeared significantly better. The interpretation of this phenomenon was correlated with the migration of the low-molecular-weight products outside due to the decrease in the section and reorganization of the morphology under the extensional stress. The

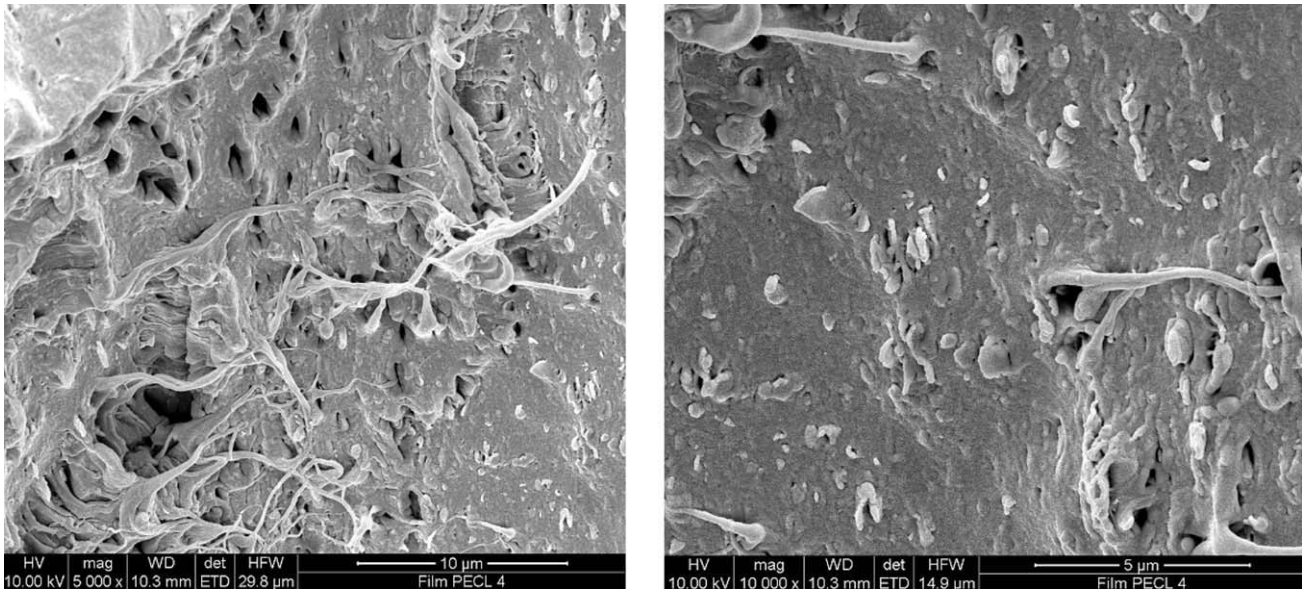

Figure 6 SEM micrographs of the PE/CL sample before film formulation at different magnifications.

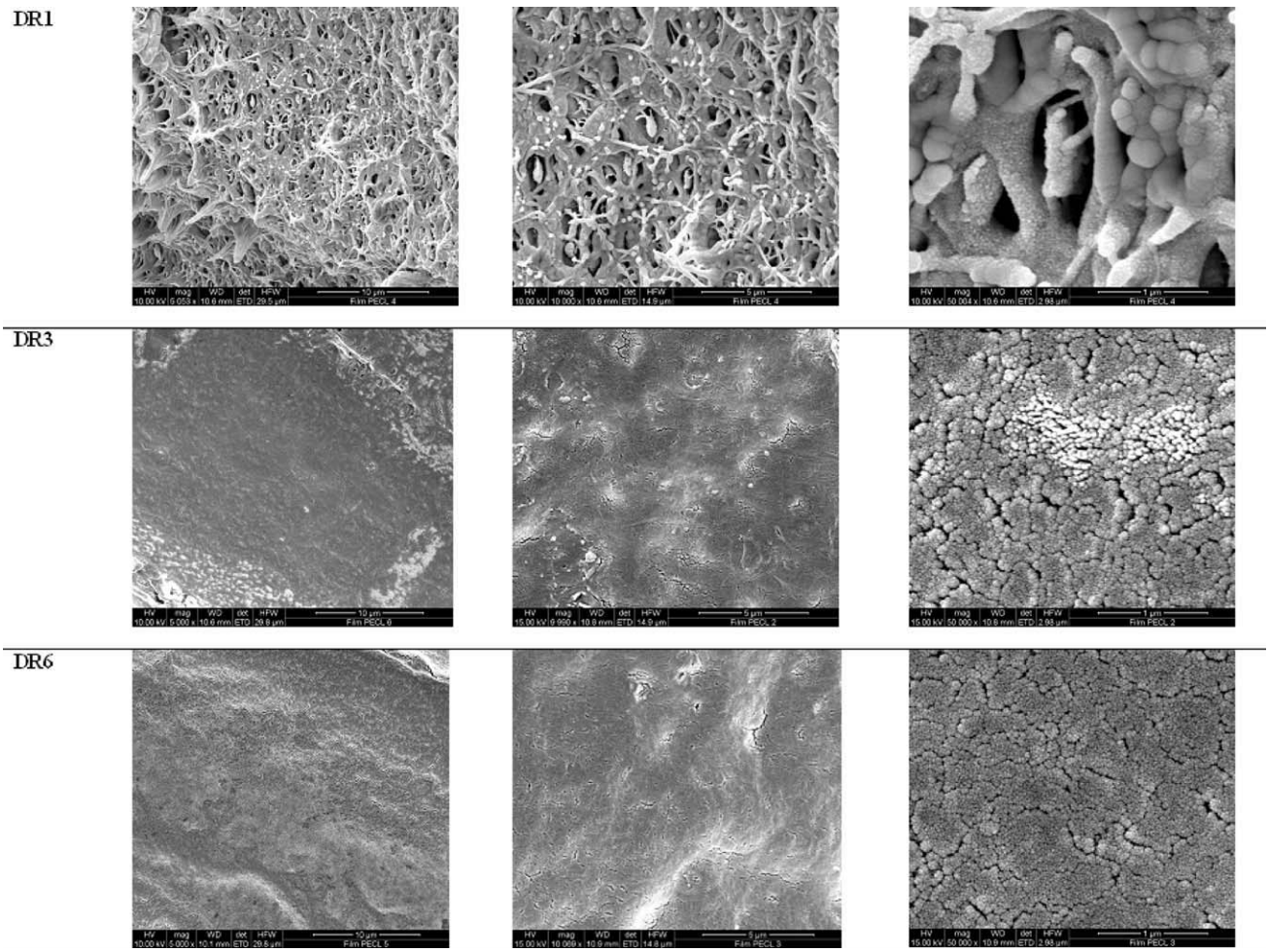

Figure 7 SEM micrographs of the PE/CL films at different DRs, that is, DRs = 1, 3, and 6, and at different magnifications.

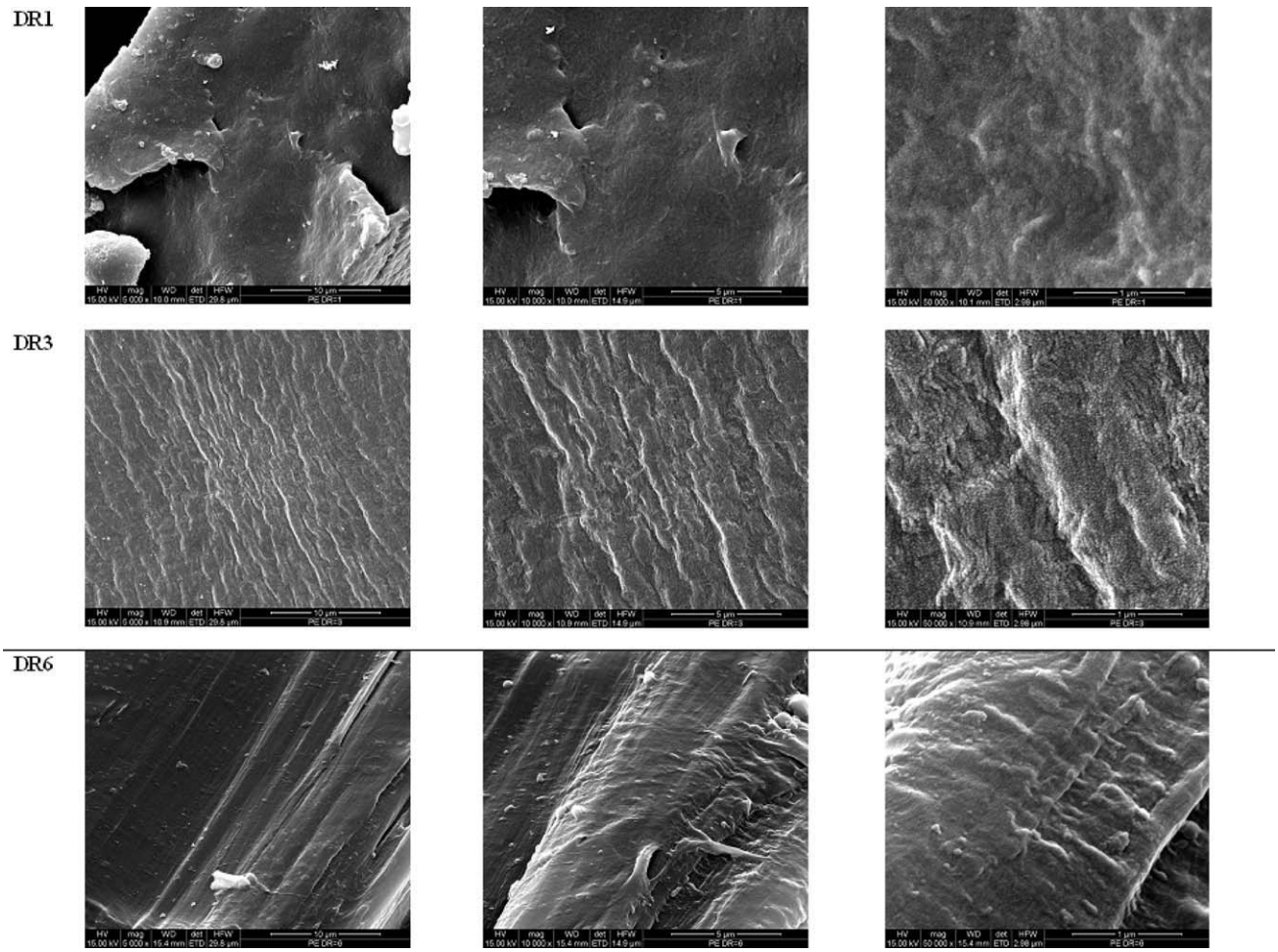

Figure 8 SEM micrographs of the PE films at different DRs, that is, DRs = 1, 3, and 6, and at different magnifications.

enhanced morphology of the PE/CL films as a function of DR was in total agreement with the obtained mechanical performances. To examine the effect of the clay presence on the morphological evaluation as a function of DR, the micrographs of the PE film (without CL; Fig. 8) were examined. The PE film with increasing DR also showed an enhanced morphology, but the morphological changes were much less that the PE/CL films. The SEM analysis clearly indicated a beneficial simultaneous effect of the clay presence and the extensional flow on the morphology modification in the PE/CL film formulation.

CONCLUSIONS

PE and PE/CL films by film blowing were formulated, and the effects of the extensional flow on the film performances were evaluated. The obtained results suggest that with the clay presence and, in particular, the increasing DR, *E* and TS increased, whereas EB and yield strain decreased. The PE/CL films, at higher DR, showed a significant ability to maintain the induced torsion deformation; that is, the twist angle as a function of the time of the PE/CL film was similar to the commercial sample one. The enhanced performances of the PE/CL film, from a twist-wrapping applicative point of view, were due to the significant obtained morphology modification upon extensional flow. Also, some beneficial synergic effect of the clay presence and the extensional flow on the morphology and, subsequently, the applicative performances was noted.

References

1. Food Packaging Technology; Coles, R.; McDowell, D.; Kirwan, M. J., Eds.; Blackwell: Oxford, 2003.
2. Materials and Development of Plastics Packaging for the Consumer Market; Giles, G. A.; Bain, D. R., Eds.; Sheffield Academic: Sheffield, England, 2000.
3. Alexandre, M.; Dubois, P. Mater Sci Eng 2000, 28, 1.
4. Polymer–Clay Nanocomposites; Pinnavaia, T. J.; Beall, G. W., Eds.; Wiley: Chichester, England, 2000.
5. Ren, J.; Silva, A. S.; Krishnamoorti, R. Macromolecules 2000, 33, 3739.
6. Dennis, H. R.; Hunter, D. L.; Chang, D.; Kim, S.; White, J. L.; Cho, J. W.; Paul, D. R. Polymer 2001, 42, 9513.

7. Krishnamoorti, R.; Ren, J.; Silva, A. S. J Chem Phys 2001, 114, 4968.
8. Ray, S. S.; Okamoto, M. Prog Polym Sci 2003, 28, 1539.
9. Incarnato, L.; Scarfato, P.; Russo, G. M.; Di Maio, L.; Iannelli, P.; Acierno, D. Polymer 2003, 44, 4625.
10. Hotta, S.; Paul, D. R. Polymer 2004, 45, 7639.
11. Fornes, T. D.; Paul, D. R. Macromolecules 2004, 37, 7698.
12. Shah, R. K.; Paul, D. R. Polymer 2006, 47, 4075.
13. La Mantia, F. P.; Dintcheva, N. T.; Filippine, G.; Acierno, D. J Appl Polym Sci 2006, 102, 4749.
14. Xie, W.; Gao, Z.; Liu, K.; Pan, W.-P.; Vaia, R.; Hunter, D.; Singh, A. Thermochim Acta 2001, 367–368, 339.
15. Fornes, T. D.; Yoon, P. J.; Paul, D. R. Polymer 2003, 44, 7545.
16. Pandey, J. K.; Reddy, K. R.; Kumar, A. P.; Singh, R. P. Polym Degrad Stab 2005, 88, 234.
17. Jang, B. N.; Wilkie, C. A. Polymer 2005, 46, 3264.
18. Dintcheva, N. T.; Al-Malaika, S.; La Mantia, F. P. Polym Degrad Stab 2009, 94, 1571.
19. Zhang, Q.; Naito, K.; Qi, B.; Kagawa, Y. J. Nanosci Nanotechnol 2009, 9, 209.
20. Tamura, K.; Yamada, H.; Yokoyama, S.; Kurashima, K. I. Am Ceram Soc 2008, 91, 3668.
21. Ariga, K.; Hill, J. P.; Lee, M. V.; Vinu, A.; Charvet, R.; Acharya, S. Sci Technol Adv Mater 2008, 9, 014109.
22. Mandal, S.; Lee, M. V.; Hill, J. P.; Vinu, A.; Ariga, K. J. Nanosci Nanotechnol 2010, 10, 21.
23. Lyngaae-Jorgensen, J. In Polymer Blends and Alloys; Folkes, M. J.; Hope, P. S., Eds.; Blackie Academic & Professional: London, 1993.
24. La Mantia, F. P.; Lo Verso, S.; Dintcheva, N. T. Macromol Mater Eng 2002, 287, 909.
25. La Mantia, F. P.; Dintcheva, N. T.; Scaffaro, R.; Marino, R. Macromol Mater Eng 2008, 293, 83.
26. Dintcheva, N. T.; Marino, R.; La Mantia, F. P. e-Polymers 2009, 054.
27. La Mantia, F. P.; Marino, R.; Dintcheva, N. T. Macromol Mater Eng 2009, 294, 575.